The Numerical and Experimental Investigation of Heat Transport and Water Infiltration in Granular Packed beds due to Supplied Hot Water (One-and Two-Dimensional Models)

P. Rattanadecho*
Faculty of Engineering, Thammasat University (Rangsit Campus),
Pathum Thani,12121, Thailand, E-mail: ratphadu@engr.tu.ac.th
***Corresponding Author**

S. Wongwises
King Mongkut University of Technology Thonburi,
91 Suksawas 48, Rat Burana, Bangkok, 10140, Thailand

Abstract

The characteristics of heat transport and water infiltration in granular packed bed due to supplied hot water are investigated experimentally and numerically. The distributions of water content and temperature are predicted for one- and two-dimensional models assuming the local thermal equilibrium among water and particles at any specific space. The predicted temperature distributions are compared with the experimental results. Most importantly, the effects of particle sizes, initial water content and supplied water flux on heat transport and flow kinetics are examined. It is found that using a larger particle size results in a faster infiltration rate and forms a wider infiltration layer, especially in the direction of gravity. However, an extension of the heated layer is not as much as that of the infiltration layer because the temperature of water infiltration gradually drops due to upstream heat transport.

Keywords: porous media, water infiltration, unsaturated flow, numerical

1. Introduction

Understanding of heat transport in granular packed bed or porous media with water infiltration due to the force of capillary suction is essential in a variety of soil science and chemical engineering applications such as temperature control of soil, recovery of geothermal energy, thermal energy storage, and various reactors in the chemical industry. Up to the present time, the related problem of water infiltration in porous media has been investigated both experimentally and numerically by many researchers [1-8]. However, few research reports have been published for heat transport in porous media with water infiltration, except the problem of permafrost [9-11] and drying technology [12-16].

The purpose of this paper is to clarify the characteristics of heat transport with water infiltration in granular packed beds experimentally and numerically. Most importantly, the effects of particle sizes, supplied water flux and initial water content on the flow kinetics are examined. The result presented here provides a basis for fundamental understanding of heat transport and water infiltration in granular materials.

2. Analysis of Unsaturated Flow in Granular Packed Bed

Figure 1 shows the schematic diagram of the Buckley-Leverett problem. This case is the unsaturated flow in granular packed bed due to supplied hot water. When the hot water is uniformly supplied at the top surface of the sample, which is initially composed of glass particles and gas, a two-phase region with the infiltration front is formed within the packed bed. In this region, co existant flow of liquid water and gas phases occurs. However, the flow due to gas phase is a dominant mechanism at the lower part.

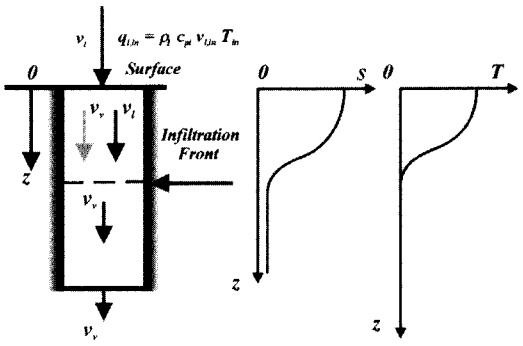

Figure 1. Schematic diagram of Buckley-Leverett problem

By conservation of mass and energy in the unsaturated granular packed bed, the governing equation of mass and energy for all phases can be derived by using a volume averaged technique [16, 17]. The main transport mechanisms that enable water infiltration during supplied hot water into the sample include;

1. Water flow is driven by capillary pressure gradient and gravity
2. The vapor is driven by the gradient of the partial pressure of the evaporating species, i.e., vapor diffusion.

Assumptions

The main assumptions involved in the formulations of the transport model are:

1.) The unsaturated granular packed bed is rigid. No chemical reactions occur in the sample.

2.) Local thermodynamic equilibrium is assumed.

3.) The gas phase is ideal in the thermodynamic sense.

4.) The contribution of convection to energy transport is included.

5.) Darcy's law holds for the liquid and gas phases.

6.) Fick's law holds for the vapor diffusion.

7.) Gravity is included for the liquid and gas phases.

8.) Permeability of liquid and gas can be expressed in terms of relative permeability.

9.) The evaporation of water and the condensation of water vapor take place simultaneously in the unsaturated flow processes. Evaporation and condensation respectively represent a heat sink and a heat source in the granular packed bed. These representations are included in the present model formulation. In a macroscopic sense, the unsaturated granular packed bed is assumed to be homogeneous and isotropic, and water does not bind to the granular beads. Therefore, the volume average model for a homogeneous and isotropic material can be used in the theoretical modeling and analysis.

Mass Conservation

The microscopic mass conservation equations for liquid and gas phases are expressed respectively, as shown below:

Liquid phase

$$\varepsilon \frac{\partial}{\partial t}[\rho_l s] + \frac{\partial}{\partial z}[\rho_l v_l] = 0 \tag{1}$$

Vapor phase

$$\varepsilon \frac{\partial}{\partial t}[\rho_v (1-s)] + \frac{\partial}{\partial z}[\rho_v v_v] = 0 \tag{2}$$

In order to complete the system of equations, the following forms of the generalized Darcy's law which are the expressions for the superficial average velocity of the liquid and gas phases are used [16]:

$$v_l = -\frac{KK_{rl}}{\mu_l}\left[\frac{\partial p_g}{\partial z} - \frac{\partial p_c}{\partial z} - \rho_l g\right] \tag{3}$$

$$v_g = -\frac{KK_{rg}}{\mu_g}\left[\frac{\partial p_g}{\partial z} - \rho_l g\right] \tag{4}$$

For the velocity of water vapor and air phases, the generalized Fick's law in the form of the partial pressure gradient of the evaporating species is applied:

$$\rho_v v_v = \rho_v v_g - \rho_g D_m \frac{\partial}{\partial z}\left(\frac{\rho_v}{\rho_g}\right) \quad (5)$$

$$\rho_a v_a = \rho_a v_g - \rho_g D_m \frac{\partial}{\partial z}\left(\frac{\rho_a}{\rho_g}\right) \quad (6)$$

where D_m is the effective molecular mass diffusion. In Eqs. (3) and (4), the capillary pressure, p_c, is related to the gas and liquid phases and can be written by:

$$p_c = p_g - p_l \quad (7)$$

Using Darcy's generalized equation (Eqs.3 and 4), mass conservation equations for liquid and gas phases (Eqs.1 and 2), are then rewritten, respectively, as:

$$\varepsilon \frac{\partial}{\partial t}[\rho_l s] - \frac{\partial}{\partial z}\left[\frac{KK_{rl}}{\nu_l}\left(\frac{\partial p_g}{\partial z} - \frac{\partial p_c}{\partial z} - \rho_l g\right)\right] = 0 \quad (8)$$

$$\varepsilon \frac{\partial}{\partial t}[\rho_v (1-s)] - \frac{\partial}{\partial z}\left[\frac{KK_{rg}}{\nu_g}\left(\frac{\partial p_g}{\partial z} - \rho_l g\right) - \rho_g D_m \frac{\partial}{\partial x}\left(\frac{\rho_v}{\rho_g}\right)\right] = 0 \quad (9)$$

Equilibrium Relations

The system of conservation equations obtained for multiphase transport mode requires constitutive equations for relative permeabilities, K_r, capillary pressure, p_c, and capillary pressure functions (Leverett functions), J. A typical set of constitutive relationships for liquid and gas system is given by:

$$K_{rl} = s_e^{\,3}, \quad K_{rg} = (1 - s_e)^3 \quad (10)$$

where s_e is the effective water saturation considered the irreducible water saturation, s_{ir}, and can be defined by:

$$s_e = \frac{s - s_{ir}}{1 - s_{ir}} \quad (11)$$

The relationship between relative permeability in each phase following Eq.10 is shown in Figure 2.

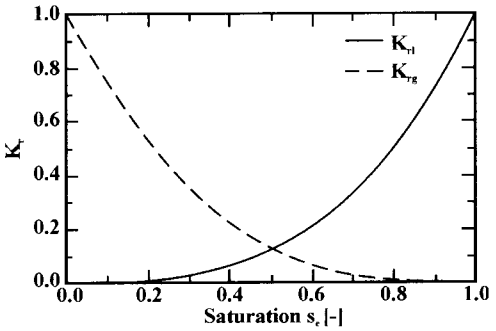

Figure 2. The relationship between, K_r and s_e

The capillary pressure, p_c, is further assumed to be adequately represented by Leverett's well know $J(s_e)$ functions. The relationship between the capillary pressure and the water saturation is defined by using Leverett functions, $J(s_e)$:

$$p_c = p_g - p_l = \frac{\sigma}{\sqrt{K/\phi}} J(s_e) \quad (12)$$

where $J(s_e)$ is correlated capillary pressure data obtained by Leverett and can be expressed follows:

$$J(s_e) = a\left(1/s_e - 1\right)^b \quad (13)$$

Further, the coefficients "a" and "b" at each condition, can be directly taken from reference [14].

Energy Conservation

Ignoring kinetic energy and pressure terms which are usually unimportant, this can be obtained from the total energy conservation of a combined solid and gas phases by invoking the assumption that the local thermodynamic equilibrium prevails among all phases. The temperature of the sample during unsaturated flow due to supplied hot water is obtained by solving the conventional heat transport equation.

$$\frac{\partial}{\partial t}\left[\left(\rho c_p\right)_T T\right] + \frac{\partial}{\partial z}\left[\left(\rho_l c_p u_l + \rho_g c_{pg} u_g\right) T\right] = \frac{\partial}{\partial z}\left[\lambda \frac{\partial T}{\partial z}\right] \quad (14)$$

where $\left(\rho c_p\right)_T$ is the effective heat capacitance of granular packed bed, λ is the effective thermal conductivity depending on

water saturation. Under thermal equilibrium conditions and using the volume average technique, the effective heat capacitance is given by:

$$\left(\rho c_p\right)_T = \rho_l c_{pl} \varepsilon s + \rho_g c_{pg} \varepsilon (1-s) + \rho_p c_{pp} (1-\varepsilon) \quad (15)$$

Based on the experimental results [14, 15] using glass beads saturated with water, the effective thermal conductivity is represented as a function of the water saturation:

$$\lambda = \frac{0.8}{1+3.78e^{-5.95s}} \quad (16)$$

Initial Condition and Boundary Conditions

Assuming that the initial effective water saturation and initial temperature are constant:

$$t<0,\ z\geq 0:\ s_e = s_0,\ T = T_0 \quad (17)$$

From experimental conditions, initial effective water saturation s_0 is given as $s_0=10^{-8}$ and the initial temperature T_0 is given as $T_0=20$ [°C]. The boundary conditions at the top and the bottom sides of granular packed bed are:

$$\begin{aligned} &t>0,\ z=0: \\ &F_{l,in} = const,\ q_{l,in} = \rho_l c_{pl} v_{l,in} T_{in} \\ &t>0,\ z=0: \\ &F_{l,in} = const,\ q_{l,in} = \rho_l c_{pl} v_{l,in} T_{in} \\ &z=Z:\ q_v = \rho_g c_{pg} v_g T_{in} \end{aligned} \quad (18)$$

Using Darcy's generalized equation, mass conservation equations for liquid and gas phases in two-dimensional form are, respectively:

$$\varepsilon\frac{\partial}{\partial t}[\rho_l s] - \frac{\partial}{\partial y}\left[\frac{KK_{rl}}{\nu_l}\left(\frac{\partial p_g}{\partial y} - \frac{\partial p_c}{\partial y}\right)\right] - \frac{\partial}{\partial z}\left[\frac{KK_{rl}}{\nu_l}\left(\frac{\partial p_g}{\partial z} - \frac{\partial p_c}{\partial z} - \rho_l g\right)\right] = 0 \quad (19)$$

$$\varepsilon\frac{\partial}{\partial t}[\rho_l(1-s)] - \frac{\partial}{\partial y}\left[\rho_l u_g - \rho_g D_m \frac{\partial}{\partial y}\left(\frac{\rho_l}{\rho_g}\right)\right] - \frac{\partial}{\partial z}\left[\rho_l w_g - \rho_g D_m \frac{\partial}{\partial z}\left(\frac{\rho_l}{\rho_g}\right)\right] = 0 \quad (20)$$

The temperature of the sample during unsaturated flow due to supplied hot water is obtained by solving the conventional heat transport equation:

$$\frac{\partial}{\partial t}\left[\left(\rho c_p\right)_T T\right] + \frac{\partial}{\partial y}\left[\left(\rho_l c_p v_l + \rho_g c_{pg} v_g\right)T\right] + \frac{\partial}{\partial z}\left[\left(\rho_l c_p w_l + \rho_g c_{pg} w_g\right)T\right] = \frac{\partial}{\partial y}\left[\lambda\frac{\partial T}{\partial y}\right] + \frac{\partial}{\partial z}\left[\lambda\frac{\partial T}{\partial z}\right] \quad (21)$$

The boundary conditions proposed for two-dimensional models are shown in Figure 3. The initial conditions are given by uniform initial temperature and water content.

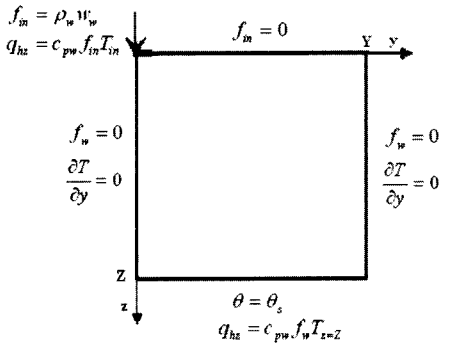

Figure 3. Two-dimensional model

3. Numerical Procedure

Corresponding to the method of finite differences based on the notion of control volumes, the generalized system of nonlinear equations are integrated over typical rectangular control volumes. After integrating over each control volume within the computational mesh, a system of nonlinear equations result, whereby each equation within this system can be cast into a numerical discretization of the generalized conservation equation. The equations of heat transport and unsaturated flow are nonlinear because, p_c, K_{rl} and K_{rg} depend on s. To solve the nonlinear equations, the Newton-Raphson iteration procedure is used for each element.

4. Experimental Apparatus

Figure 4 shows the experimental apparatus for measuring capillary pressure against water saturation in a granular packed bed. A percolator with dimension of 2300 mm in height having glass filter at the bottom is connected with a glass manometer. The test glass beads forming

the porous matrix is placed in the percolator. Capillary pressure is calculated by measuring the suction pressure obtained from the difference of water level. Water saturation in a granular packed bed is obtained by measuring the quantity of water draining.

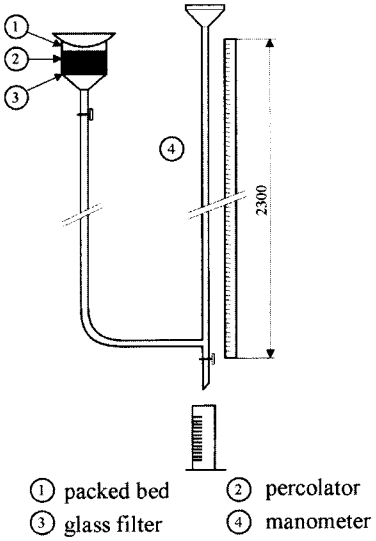

Figure 4. Experimental apparatus for measuring capillary pressure

Figure 5 shows the experimental apparatus for measuring the permeability against water flow rate. The test column with inner diameter of 50 mm, is made of acrylic resin. Spherical soda lime glass beads with average sizes of 0.15, 0.2, 0.25 and 0.4 mm are used as a sample of granular packed beds. The permeability in granular packed beds saturated with water is measured from the experiments of the steady water flow setting on the constant water head.

Figure 6 shows the experimental apparatus for one-dimensional heat transport in granular packed bed with unsaturated flow. The test column, 60 mm inner diameter and 400 mm in height, is made of acrylic resin and equipped with stainless steel screen at the bottom of the bed to prevent the movement of particles. Spherical soda lime glass beads with average sizes of 0.15 and 0.4 mm, are used as a sample of granular packed beds.

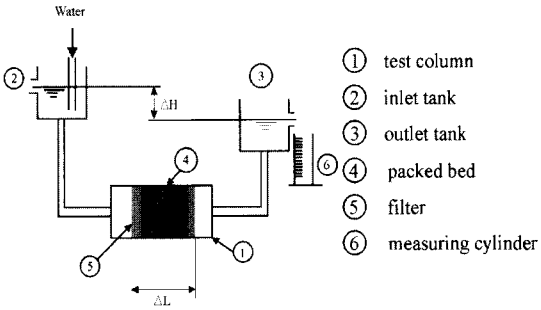

Figure 5. Experimental apparatus for measuring permeability

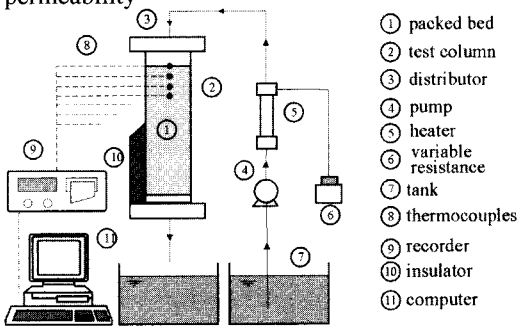

Figure 6. Experimental apparatus for measuring heat transport and unsaturated flow in a granular packed bed

The water pumped from a tank is heated at a certain temperature in a heating section and is uniformly supplied at the top of granular packed bed through a distributor. The test column is covered with insulation to reduce heat loss. The distributions of temperature within granular packed beds are measured with Cu-C thermocouples with diameter of 0.1 mm. These thermocouples are set up at 20 mm interval along the axis of granular packed bed. The distributions of temperature are recorded by a data logger connected to a computer. The position of infiltration front in the packed bed is determined by interpolating the prescribed temperature from the adjacent thermocouple reading.

Initially, the water content and the temperature are uniform within the packed bed. The experiments are carried out for the conditions of constant supplied water flux and temperature of the supplied hot water. During the experimental processes, the uncertainty of our data might come from human errors and from variations of ambient humidity and temperature.

The uncertainty in flow kinetics is assumed to result from errors in the measured supplied water flux. The calculated flow kinetic uncertainties in all tests are less than 2.95 percent. The uncertainly in temperature is assumed to result from errors in measured input power, ambient temperature and ambient humidity. The calculated uncertainty associated with temperature is less than 2.45 percent.

5. Result and Discussion

One-Dimensional Heat and Unsaturated Flow

Figure 7 shows the distributions of water saturation and temperature at various elapsed times as a parameter of supplied water flux, which corresponds to the diameter of 0.15 mm. It is found that a greater supplied water flux in the packed bed corresponds to a higher water saturation and forms a wider infiltration layer, i.e., infiltration front. Here, the main transport mechanisms that enable fluid movement are: liquid flow driven by capillary pressure gradient and gravity while the vapor is driven by molecular diffusion. Liquid phase migration is related to capillary pressure gradient as well as temperature (which corresponds to that of surface tension, as referred to in Eq.12), whereas the vapor phase is driven by the gradient of the partial pressure of the evaporating species. The temperature in the granular packed bed rises due to water infiltration, but the heated layer does not extend as much as the infiltration layer. This means that heat transport hardly occurs in the layer close by the infiltration front because the temperature of water infiltration there has already dropped due to upstream heat transport. The predicted results for the temperature distributions are in agreement with the experimental results.

Figure 8 shows the influence of particle sizes on the distributions of water saturation and temperature under the same supplied water flux. The results show that a larger particle size leads to a faster infiltration rate and forms a wider infiltration layer. The heated layer also expands somewhat with a larger particle size. It is evident from the figure that the discrepancy of the heated layers is smaller compared to the infiltration layers.

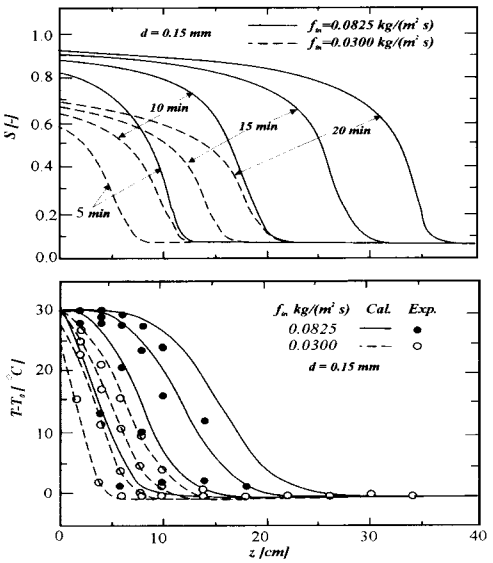

Figure 7. Distribution of water saturation and temperature profiles at various elapsed times as a parameter of supplied water flux

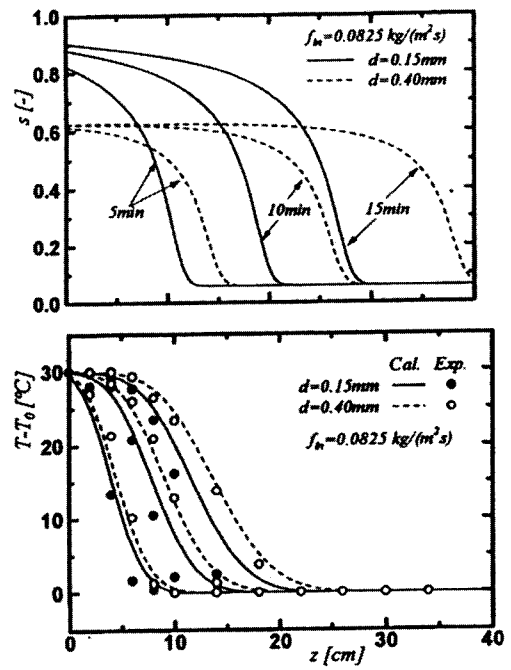

Figure 8. Distribution of water saturation and temperature profiles at various elapsed times as a parameter of particle sizes

To clarify heat transport in a granular packed bed, the distributions of the rate of heat storage per unit volume at different times are

shown in Figure 9. In the early stage of unsaturated flow, the maximum rate of heat storage is more intense close to the leading edge of the packed bed. As unsaturated flow progresses, the value of the maximum rate decreases and its position gradually moves to the downstream side, resulting in the formation of a wider layer.

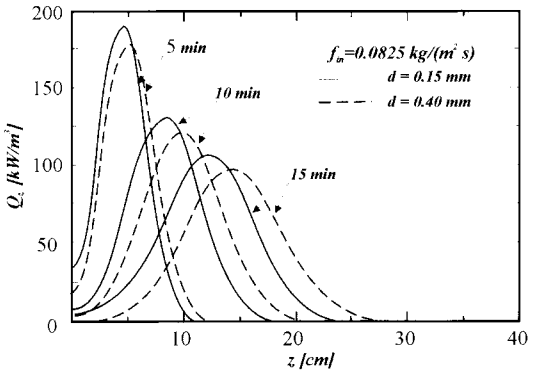

Figure 9. Distribution of rate heat storage per unit volume at various elapsed times as a parameter of particle sizes

Two-Dimensional Heat and Water Transport

The two-dimensional heat and water infiltration in y- and z-directions (1/4 of symmetrical plan) will now be discussed with the aids of Figures 10-17. Figure 10-13 shows the effect of particle size on water infiltration under a constant supplied water flux. In the early stage of infiltration, the infiltration layer expands uniformly in both y- and z-directions because capillary pressure has more influence than a gravity potential. As water infiltration progresses, the gravitational effect becomes superior to the capillary pressure and the infiltration layer expands wider in the z-direction which is the direction of gravity. However, the infiltration front in the case of small particle size expands wider in the y-direction in comparison with a larger particle size, due to the stronger effect of the capillary pressure.

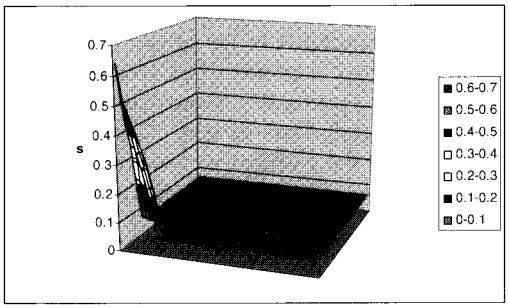

Figure 10. Water saturation profile in case of small particle size (10 min)

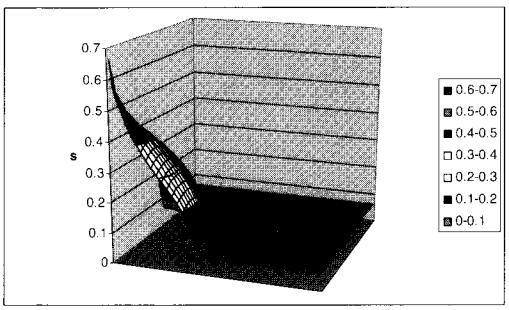

Figure 11. Water saturation profile in case of small particle size (60 min)

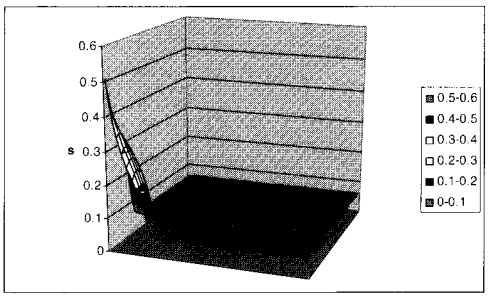

Figure 12. Water saturation profile in case of larger particle size (10 min)

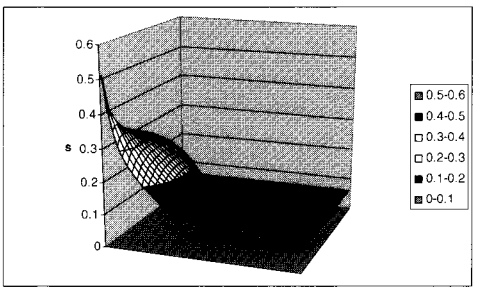

Figure 13. Water saturation profile in case of larger particle size (60 min)

Figures 14-17 show the effect of particle size on the expansion of the heated layer due to infiltration of supplied hot water, which corresponds to the conditions shown in the previous case. The heated layer expands somewhat in the z-direction at a larger particle size, but the effect of particle size on the expansion of the heated layer is smaller as compared to the infiltration layer. It is found that the heated iayer are always wider in the z-direction and narrower in the y-direction for a larger particle size.

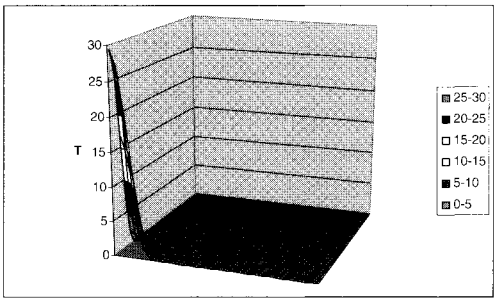

Figure 14. Temperature profile in case of small particle size (10 min)

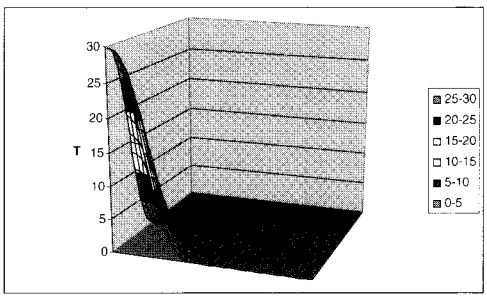

Figure 15. Temperature profile in case of small particle size (60 min)

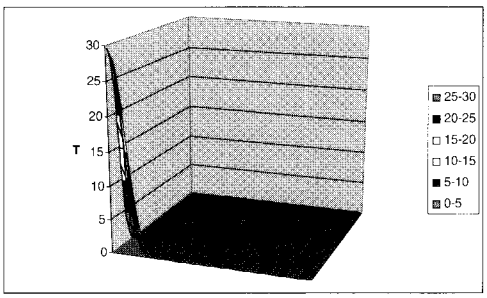

Figure 16. Temperature profile in case of large particle size (10 min)

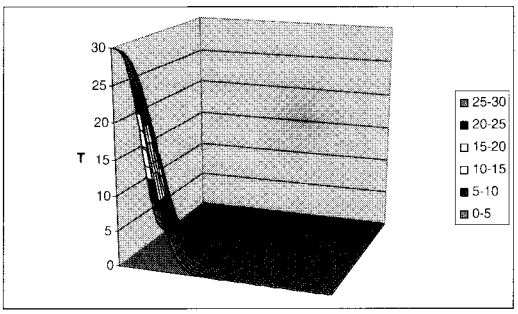

Figure 17. Temperature profile in case of large particle size (60 min)

6. Conclusions

Based on one and two-dimensional models where there is thermal equilibrium between the water and the matrix at any specific space, the heat transport in granular packed bed with unsaturated flow is investigated. The following are the conclusions of this work:

1.) A generalized mathematical model of heat transport with water infiltration within a packed bed is proposed. It is used successfully to describe the flow phenomena under various conditions.

2.) When comparing the distribution profiles between heated layer and infiltration layer, it is observed that the heated layer does not extend as much as the infiltration layer. This means that heat transport hardly occurs in the layer close to the infiltration front because the temperature of water infiltrating gradually drops, due to upstream heat transport. Furthermore, the effect of particle size on the discrepancy of heated layers is smaller, compared to that of the water content layers.

3.) It is found that the gravity and capillary pressure have clearly exhibited influence on the infiltration and heated layers.

4.) It is possible to use the present model for analysis of numerous other applications (e.g. temperature and moisture movement in the ground, the stability of buried electrical cables and underground soil heating).

Nomenclature

A	coefficient in Table 1
B	coefficient in Table 1
c_p	specific heat, (J/kg.K)
d	particle diameter, (m)
D_m	effective molecular mass diffusion [m^2/s]

f supplied water flow rate, $(kg/m^2).s$
g gravitational acceleration, (m/s^2)
h_{fv} specific heat of vaporization, (J/kg)
K permeability, (m^2)
K_r relative permeability
$\dot{n}$ phase change term, $(kg/m^2).s$
p pressure, (pa)
q heat flux, (W/m^2)
Q rate of heat storage per unit volume, (kW/m^3)
s water saturation
t time, (s)
T temperature, (°C)
V velocity, (m/s)

Greek letters

ε porosity, (m^3/m^3)
ρ density, (kg/m^3)
λ effective thermal conductivity, (W/mK)
μ dynamic viscosity of liquid, (Pa s)
σ surface tension, (N/m)

Subscripts

0: initial
a: air
c: capillary
e: effective
g: gas
in: input
ir: irreducible
l: liquid
p: particle
r: relative
v: vapor
x: coordinates

Acknowledgments

The authors are pleased to acknowledge the Thailand Research Fund (TRF) for supporting this research work. We are also grateful to Prof. K. Aoki of the Nagaoka University of Technology for valuable recommendations in this research area.

References

[1] Campbell, G.S., Soil Physics with Basic, Elsevier, New York., 1985.
[2] Bear, J., Dynamics of Fluids in Porous Media, Elsevier, New York, 1972.
[3] Haverkamp, R., Vauclin, M., Touma, J., Wierenga, P.J. and Vachaud, G., A Comparison of Numerical Simulation Models for One-dimensional Infiltration, Soil Sci. Soc. Am. J., Vol. 41, pp. 285-294, 1977.
[4] Parlange, J.Y., Theory of Water-movement in Soils, One-dimensional Infiltration, Soil Sci, Vol. 111, pp. 170-174, 1972.
[5] Schrefler, B. A. and Zhan Xiaoyong, A fully Coupled Model for a Water Flow and Air Flow in Deformable Porous Media, Water Resources Research, Vol. 29, pp. 155-167, 1993.
[6] Thomas, H.R., and King, S.D., Coupled Temperature/capillary Potential Variations in unsaturated soil, J. Engrg. Mech. ASCE., Vol. 117(11), pp. 2475-2491, 1991.
[7] Thomas, H.R., and Sansom, M.R Fully Coupled Analysis of Heat, Moisture, and air Transfer in Unsaturated soil, J. Engrg. Mech. ASCE., Vol. 117(11), pp. 2475-2491, 1995.
[8] Kutsovky, Y.E., Scriven, L.E., Davis, H.T., and Hammer, B.E., NMR Imaging of Velocity Profiles and Velocity Distribution in Packed Beads, Phys. Fluids, 8, 863, 1996.
[9] Harlan, R.L., Analysis of Coupled Heat-Fluid Transfer in Partially Frozen Soil, Water Resources Research, Vol. 9, pp. 1314-1323, 1973.
[10] Kennedy, G.F., and Lielmezes, J., Heat and Mass Transfer of Freezing Water-soil Systems, Water Resources Research, Vol. 9, pp. 395-400, 1973.
[11] Guymon, G.L., and Luthin, J.N., A Coupled Heat and Moisture Transport Model for Arctic Soils, Water Resources Research, Vol. 10, pp. 995-1001, 1974.
[12] Ben Nasrallah, S., and Perre, P., Detailed Study of a Model of Heat and Mass Transfer During Convective Drying of Porous Media, Int. J. Heat and Mass Transfer, Vol. 31, pp. 957-967, 1988.
[13] Rogers, J.A., and Kaviany, M., Funicular and Evaporative-front Regimes in Convective Drying of Granular Beds, Int. J. Heat and Mass Transfer, Vol. 35, pp. 469-479, 1992.
[14] Ratanadecho, P., Aoki, K., and Akahori, M., Experimental and Numerical Study of Microwave Drying in Unsaturated Porous Material, Int. Commun. Heat Mass Trans., Vol. 28, pp. 605-616, 2001.

[15] Ratanadecho, P., Aoki, K., and Akahori, M., A Numerical and Experimental Study of Microwave Drying Using a Rectangular wave Guide, Drying Technology International Journal, Vol. 19, pp. 2209-2234, 2001.

[16] Ratanadecho, P., Aoki, K., and Akahori, M., Influence of Irradiation Time, Particle Sizes and Initial Moisture Content During Microwave Drying of Multi-layered Capillary Porous Materials, ASME J. Heat Transfer, Vol. 124, pp. 151-161, 2002.

[17] Kaviany, M., and Mittal, M., Funicular State in Drying of Porous Slab, Int. J. Heat and Mass Transfer, Vol. 30, pp. 1407-1418, 1987.